

static potential was not considered. The Co atom was regarded as a C atom because of the lack of reliable parameters for the Co atom. The results are listed in Table 7.

The potential energy for the *S-S-pea(I)* complex at the final stage at 296 K was -190 kJ mol^{-1} , which is about 9 kJ mol^{-1} higher than that of the initial structure at the same temperature. The cause of this difference in packing potential energy is mainly not the repulsion by the inverted ce group but the loss of the attraction by the vacancy induced by the reaction. The packing potential energy represents the enthalpy term in the total energy. The entropy term associated with the racemization of the ce group is about 1.7 kJ mol^{-1} at room temperature and cannot override the gap in the enthalpy term at the ground state though the replacement was carried out for the Co atom. However, the entropy term may be a driving force at the excited state.

The packing potential energy was calculated for the final structure of *S-S-pea(I)* using the original cell dimensions. The value was -160 kJ mol^{-1} , which is 30 kJ mol^{-1} higher than that in the final cell. This energy was released by the cell change.

The packing potential energy was also calculated for the imaginary racemic structure of an (*S* + *R*)-*S-pea(II)* crystal at 296 K. This structure was generated by inverting half of the methyl group in the ce group around the cyano group. The packing potential energy for this structure was calculated to be $+543 \text{ kJ mol}^{-1}$. This value is about 755 kJ mol^{-1} higher than the chiral *S-S-pea(II)* structure at 296 K. The racemization seems to be impossible for the *S-S-pea(II)* crystal.

Table 7. Packing potential energy (PPE; kJ mol^{-1}) of *S-S-pea(I)* and *S-S-pea(II)* complexes

<i>T</i> (K)	S-S-pea(I)				Final	S-S-pea(II)	
	Initial	Initial	Initial	Initial		Initial	Initial
223	253	296	333	296	223	296	
PPE (kJ mol^{-1})	-201	-199	-199	-196	-190	-212	-212

This work was partly supported by a Grant-in-Aid for Scientific Research from the Ministry of Education, Science and Culture, Japan.

References

- GAVEZZOTTI, A. (1983). *J. Am. Chem. Soc.* **105**, 5220–5225.
- KURIHARA, T., UCHIDA, A., OHASHI, Y., SASADA, Y., OHGO, Y. & BABA, S. (1983). *Acta Cryst.* **B39**, 431–437.
- Molecular Structure Corporation (1985). *TEXSAN. TEXRAY Structure Analysis Package*. MSC, 3200 Research Forest Drive, The Woodlands, TX 77381, USA.
- OHASHI, Y. (1988). *Acc. Chem. Res.* **21**, 268–274.
- OHASHI, Y. & SASADA, Y. (1977). *Nature (London)*, **267**, 142–144.
- OHASHI, Y., SASADA, Y. & OHGO, Y. (1978). *Chem. Lett.* pp. 743–746.
- OHASHI, Y., SASADA, Y., TAKEUCHI, S. & OHGO, Y. (1980). *Bull. Chem. Soc. Jpn*, **53**, 1501–1509.
- OHASHI, Y., YANAGI, K., KURIHARA, T., SASADA, Y. & OHGO, Y. (1981). *J. Am. Chem. Soc.* **103**, 5805–5812.
- OHGO, Y., TAKEUCHI, S., NATORI, Y., YOSHIMURA, J., OHASHI, Y. & SASADA, Y. (1981). *Bull. Chem. Soc. Jpn*, **54**, 3095–3099.
- OSANO, Y. T., DANNO, M., UCHIDA, A., OHASHI, Y., OHGO, Y. & BABA, S. (1991). *Acta Cryst.* **B47**, 702–707.
- SEKINE, A. & OHASHI, Y. (1991). *Bull. Chem. Soc. Jpn*, **64**, 2183–2187.
- SHELDRIK, G. M. (1976). *SHELX76*. Program for crystal structure determination. Univ. of Cambridge, England.
- TAKENAKA, Y., OHASHI, Y., TAMURA, T., UCHIDA, A., SASADA, Y., OHGO, Y. & BABA, S. (1993). *Acta Cryst.* **B49**, 272–277.
- TOMOTAKE, Y., UCHIDA, A., OHASHI, Y., SASADA, Y., OHGO, Y. & BABA, S. (1985). *Isr. J. Chem.* **25**, 327–333.

Acta Cryst. (1993). **B49**, 859–867

Crystal Chemistry and Physical Properties of a Series of *N*-Substituted (Thio)Morpholinium Di-7,7,8,8-tetracyano-*p*-quinodimethanides

BY RUDY J. J. VISSER, JAN L. DE BOER AND AAFJE VOS

Materials Science Centre, Department of Inorganic Chemistry, Nijenborgh 4, 9747 AG Groningen, The Netherlands

(Received 7 April 1992; accepted 28 January 1993)

Abstract

Crystal structures of a series of the title compounds are compared. Classes I, II and II' with 2, 4 and 8 tetracyanoquinodimethane (TCNQ) moieties per translation period, respectively, are distinguished.

For class I a subclassification is made according to: the number of inequivalent stacks (1 or 2); cation disorder [dynamic (*d*) or static (*s*)]; and chain directions [parallel (*p*) or crossed (*c*)]. Crystals of classes II and II' appear to be of type (1,*d,p*). Disorder of the cations is a frequent phenomenon. Generally,

changes in the ordering of the cations play an important role in the phase transitions. Magnetic susceptibility curves $\chi(T)$ turn out to be different for the various (sub)classes. Within each (sub)class the electrical conductivity decreases with increasing calculated band gap. A quantitative interpretation of the electrical transport properties is considered impossible because of the interaction between charge carriers and the *dynamic* lattice as a whole. Large unpredictable variations in crystal structure are observed for chemically small modifications of the cations. Therefore, it is concluded that crystals with *a priori* desired physical properties cannot be designed in a systematic way.

Introduction

The 1:2 charge-transfer complexes of substituted (thio)morpholinium cations $RR'(T)M^+$ ($R = -H$ or $-alkyl$; $R' = -alkyl$) and the electron acceptor 7,7,8,8-tetracyano-*p*-quinodimethane (TCNQ) contain segregated quasi-one-dimensional TCNQ stacks. Therefore, these complexes form a class of low-dimensional materials. Changes in the cations can be introduced by replacing oxygen with sulfur and/or by variation of R and R' . The influence of such changes on crystal packing, phase transitions and electronic properties has been the object of extensive research. Structures of a series of compounds determined in Groningen have been published in separate papers. In the present paper, the structures are compared and a discussion of the physical properties is given. The abbreviated nomenclature for the cations, e.g. MEM for *N*-methyl-*N*-ethylmorpholinium and DMTM for *N,N*-dimethylthiomorpholinium, is explained in the *Introduction* to the paper by Visser, Bouwmeester, de Boer & Vos (1990a). For the cations occurring in the present paper, the short and full names are listed in Table 1. Detailed descriptions of the stacks and of the packing in the corresponding crystals are given in the appropriate references. Some figures showing characteristic crystal packing are given again here.

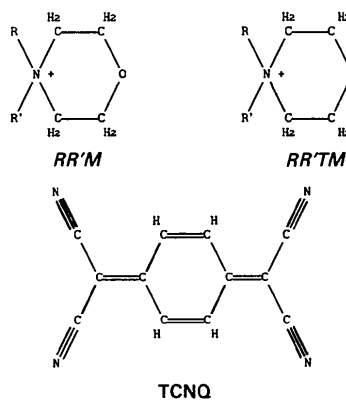


Table 1. *Short and full names of the cations in alphabetical order*

The order of R and R' in the names used in this paper is not alphabetic, the smaller group is given first. For $R = -H$, the systematic IUPAC name is preceded by '*N*-Hydrogen-':

Short name	Full name	IUPAC name
DEM	<i>N,N</i> -Diethylmorpholinium	<i>N,N</i> -Diethylmorpholinium
DMM	<i>N,N</i> -Dimethylmorpholinium	<i>N,N</i> -Dimethylmorpholinium
DMTM	<i>N,N</i> -Dimethylthiomorpholinium	<i>N,N</i> -Dimethylthiomorpholinium
EBM	<i>N</i> -Ethyl- <i>N</i> -butylmorpholinium	<i>N</i> -Butyl- <i>N</i> -ethylmorpholinium
EBTM	<i>N</i> -Ethyl- <i>N</i> -butylthiomorpholinium	<i>N</i> -Butyl- <i>N</i> -ethylthiomorpholinium
HBTM	<i>N</i> -Hydrogen- <i>N</i> -butylthiomorpholinium	<i>N</i> -Butylthiomorpholinium
HEM	<i>N</i> -Hydrogen- <i>N</i> -ethylmorpholinium	<i>N</i> -Ethylmorpholinium
HMM	<i>N</i> -Hydrogen- <i>N</i> -methylmorpholinium	<i>N</i> -Methylmorpholinium
MBM	<i>N</i> -Methyl- <i>N</i> -butylmorpholinium	<i>N</i> -Butyl- <i>N</i> -methylmorpholinium
MBTM	<i>N</i> -Methyl- <i>N</i> -butylthiomorpholinium	<i>N</i> -Butyl- <i>N</i> -methylthiomorpholinium
MEM	<i>N</i> -Methyl- <i>N</i> -ethylmorpholinium	<i>N</i> -Ethyl- <i>N</i> -methylmorpholinium
METM	<i>N</i> -Methyl- <i>N</i> -ethylthiomorpholinium	<i>N</i> -Ethyl- <i>N</i> -methylthiomorpholinium
MPM	<i>N</i> -Methyl- <i>N</i> -propylmorpholinium	<i>N</i> -Methyl- <i>N</i> -propylmorpholinium

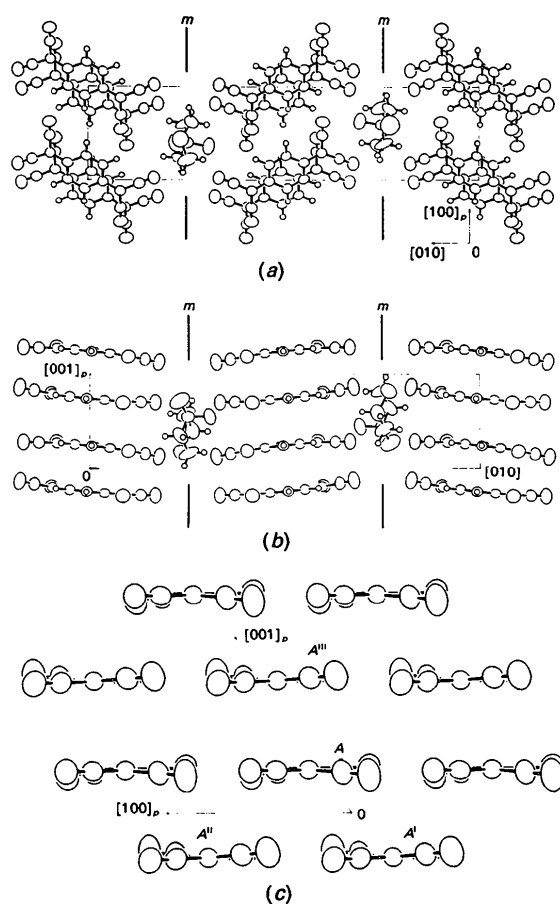


Fig. 1. Projections of the room-temperature structure of DMTM(TCNQ)₂ (from Visser, de Boer & Vos, 1990b). For each DMTM group disordered around the mirror plane, only one of the two molecules is shown; the subscript p denotes the projected direction. (a) Along [001] onto the plane perpendicular to [001]; (b) along [100] onto the plane perpendicular to [100]; (c) normal projection of the layer ('sheet') of TCNQ molecules between two successive mirror planes along the molecular axis L defined in Fig. 2. Shortest $N \cdots H$ distances between neighbouring stacks in the sheet are 2.63 (1) Å.

Table 2. Structural characteristics of $[RR'(T)M](TCNQ)_2$ compounds

Classes I, II and II' have 2, 4 and 8 TCNQ's per stack period, respectively; subclasses are distinguished by the number of inequivalent stacks ($nr = 1$ or 2), disorder [dynamic (d) or static (s)] and chain directions [parallel (p) or crossed (c)]; T is the temperature of structure determination, where RT is room temperature; Z is the number of formula units per cell; in the 'Stack period' column, different letters indicate inequivalent molecules; the $t(i)$ are calculated values (eV) of transfer (overlap) integrals; $\Delta\rho$ (e) = $(1/2)[\rho(A) - \rho(B)]$ (e.s.d. in parentheses), with $\rho(A) + \rho(B) = 1$; the references are to X-ray or neutron diffraction work.

Class I	Cation	T (K)	Space group	Z	Stack period	$t(1)^b$	$t(2)$	$\Delta\rho$	Disordered groups	Reference	
(1, d,p)	MEM	113	$P1$	1	$A-B-$			0.12 (3)		1	
	MEM	RT	$P1$	1	$A-B-$	0.20	0.06	0.11 (12)	MEM (see Table 4)	2	
	MEM	323	$P1$	1	$A-B-$	0.19	0.06	?	MEM	2	
	MEM	348	$P\bar{1}$	1	$A-A-$	0.17	0.16		MEM, around $\bar{1}$	3	
	MBTM	RT	$P\bar{1}$	2	$A-B-$	0.17	0.17	0.14 (10)	Butyl	4	
	METM	RT	$P\bar{1}$	2	$A-B-$	0.18	0.18	0.17 (2)		4	
	DMM(II) ^a	RT	$P\bar{1}$	2	$A-B-$	0.15	0.11	-0.36 (4)	DMM, chair to chair	5	
	DMM(II) ^a	99	$P\bar{1}$	2	(c)				Long-range order DMM	6	
	DMM(I) ^a	RT	$P2_1/m$	2	$A-A-$	0.18	0.06		DMM, around m	7	
	DMTM	RT	$P2_1/m$	2	$A-A-$	0.18	0.04		DMTM, around m	8	
	(1, d,c)	HMM	RT	$P4_1$	4	$A-B-$	0.17	0.16	0.19 (6)	Large U 's	9
	(1, s,p)	HBTM	RT	$P\bar{1}$	1	$A-A-$	0.17	0.15	Locally $\neq 0$	HBTM, around $\bar{1}$	10
	(2, d,p)	MBM	RT	$P\bar{1}$	2	$A-A-$	0.17	0.17	0.02 (5)	Methyl, butyl	11
						$B-B-$	0.17	0.15			
	(2, d,c)	MPM	RT	$P\bar{1}$	2	$A-A-$	0.18	0.16	0.04 (2)		11
						$B-B-$	0.20	0.12			
$A-A-$						0.19	0.04	0.02 (4)	DEM	12	
					$B-B-$	0.22	0.03				
Class II	Cation	T (K)	Space group	Z	Stack period	$t(AB)^d$	$t(BB)$	$t(AA)$	$\Delta\rho$	Disordered groups	Reference
(1, d,p)	MEM	6	$P1$	2	$A-B-C-D-$?		13
	HEM	RT	$P\bar{1}$	2	$A-B-B-A-$	0.19	0.19	0.10	-0.21 (2)	HEM, two positions	14
	EBTM	RT	$P\bar{1}$	2	$A-B-B-A-$	0.21	0.13	0.02	-0.17 (3)		15
	EBM	RT	$P2_1/c$	4	$A-B-B-A-$	0.16	0.17	0.15	-0.01 (4)		15
Class II'	Cation	T (K)	Space group	Z	Stack period	$t(i)$	$\Delta\rho$			Reference	
(1, d,p)	DMM(I α) ^a	95	$P2_1/c$	8	Octameric	0.05-0.20	(f)			16	

Notes: (a) (I) = monoclinic, (II) = triclinic form with one low-temperature modification for (II) and two low-temperature modifications (I α) and (I β) for (I) [the crystal structure of (I β) is unknown and it is not treated here]. (b) $t(1) \geq t(2)$, for $t \geq 0.11$ (distorted) type-I or type-II (in bold type) overlap (types defined in Fig. 2). (c) Incommensurable modulation. (d) $t(BA) = t(AB)$ because of inversion symmetry. (e) $C-D$ shifted with respect to $A-B$ by 0.20 (3) Å parallel to TCNQ planes. (f) Charges vary from 0.42 to 0.58 (3)e.

References: (1) Bosch & van Bodegom (1977); (2) van Bodegom (1981); (3) van Bodegom & Bosch (1981); (4) Visser, Bouwmeester, de Boer & Vos (1990a); (5) Visser (1984); (6) Steurer, Visser, van Smaalen & de Boer (1987); (7) Kamminga & van Bodegom (1981); (8) Visser, de Boer & Vos (1990b); (9) Visser, de Boer & Vos (1990c); (10) Visser, van Smaalen, de Boer & Vos (1990); (11) Visser, de Boer, & Vos (1990a); (12) Morssink & van Bodegom (1981); (13) Visser, Oostra, Vettier & Voiron (1983); (14) van Bodegom & de Boer (1981); (15) Visser, Bouwmeester, de Boer & Vos (1990b); (16) Middeldorp, Visser & de Boer (1985).

Crystal chemistry

Structural characteristics

Fig. 1 shows the structure of DMTM(TCNQ)₂ at room temperature. It is easy to see that the crystal contains TCNQ stacks along the c axis. DMTM(TCNQ)₂ exemplifies the characteristic situation for the present compounds where the $RR'(T)M^+$ cations are shaped such that they pack alongside more than one TCNQ group in a stack. Therefore, genuinely regular stacks, in which all TCNQ molecules are translationally equivalent, do not occur in the $[RR'(T)M](TCNQ)_2$ salts.

Characteristic features of the crystal structures are listed in Table 2. Classes I, II and II' with 2, 4 and 8 TCNQ moieties per translation period along the stack, respectively, are distinguished. For class I a subclassification is made according to: (1) the number (nr) of inequivalent stacks (1 or 2); (2) the character of the cation disorder [dynamic (d) or static (s)]; and (3) the directions of the stacks [parallel (p) or crossed (c)]. With this classification, the available

crystals in classes II and II' appear to be of the (1, d,p) type.

Each crystal structure is identified by the short name of its cation (with modification label when necessary) and the temperature of its structure determination. Note that there are two modifications for DMM(TCNQ)₂, a monoclinic form DMM(TCNQ)₂(I), and a triclinic form, DMM(TCNQ)₂(II), each having at least one low-temperature phase transition [footnote (a) to Table 2]. The space group and Z are followed by the characteristics of the independent stacks (one for $nr = 1$ and two for $nr = 2$). In the 'stack period' column, inequivalent TCNQ molecules are represented by different letters. Stacks with equivalent molecules within the stack period contain inversion centres. An example is the room-temperature structure DMM(TCNQ)₂(I), where all TCNQ molecules are indicated by A . In the room-temperature structure DMM(TCNQ)₂(II) with inversion centres *between* neighbouring stacks, molecules A and B alternate in the stack. In the subsequent columns, the overlaps of successive molecules i

and $i + 1$ in a stack are characterized by the transfer integrals $t(i)$, taken from van Smaalen & Kommandeur (1985). According to their approximations, the transfer integrals are proportional to the overlap integrals between the lowest unoccupied molecular orbitals $\Phi(i)$ and $\Phi(i + 1)$ of the molecules considered:

$$t(i) = C \int \Phi(i; \mathbf{r}) \Phi(i + 1; \mathbf{r}) d\mathbf{r}. \quad (1)$$

For the present 1:2 compounds the constant C is chosen such that $t(1)$ of MEM(TCNQ)₂ at room temperature adopts the value 0.195 eV, deduced by an approximate theoretical method from the polarized-infrared-reflectance spectra by Rice, Yartsev & Jacobsen (1980). Overlaps with $t \geq 0.11$ are of the (distorted) type-I or type-II modes defined in Fig. 2; in the case of a type-II overlap, t is given in bold type. The t values illustrate that the compounds exhibit strong variation in the degree of dimerization or tetramerization of the stacks. At room temperature, pronounced dimeric stacks are observed in MEM(TCNQ)₂, DMM(TCNQ)₂(I), DMTM(TCNQ)₂ and DEM(TCNQ)₂. In EBTM(TCNQ)₂ almost isolated tetramers are found.

With the assumption of complete charge transfer from the cations to TCNQ, two TCNQ moieties share a charge of 1 e. In general this charge is unevenly distributed over two inequivalent molecules A and B . The charge differences

$$\Delta\rho = (1/2)[\rho(A) - \rho(B)], \quad (2)$$

given in the column ' $\Delta\rho$ ' of Table 2, are calculated from the bond lengths according to Flandrois &

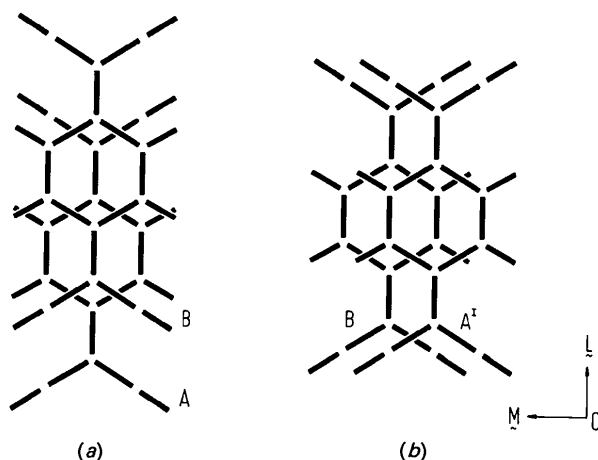
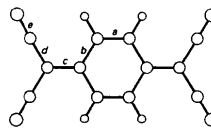


Fig. 2. Favourable overlap modes for TCNQ stacks. (a) Ring-external bond or type-I overlap; (b) ring-ring or type-II overlap. A right-handed orthonormal inertial system of axes for the TCNQ quinodimethane skeleton is defined by L , M , N (N perpendicular to plane). Idealized displacement vectors (N component representative for room-temperature structures): $\nu_{i, i+1}(I) = 2.10L + 0.00M + 3.25N$, $\nu_{i, i+1}(II) = 0.00L + 1.20M + 3.25N$. Shortest intermolecular $C \cdots C$ distance 3.30 Å.

Table 3. Mean bond lengths (Å) and charges ρ (e) of the TCNQ molecules in DMM(TCNQ)₂(II) at room temperature



The standard deviation of a , b , c , d and e of TCNQ's A and B , calculated as the mean of the standard deviations of the individual bonds from which each quantity is derived, is 0.004 Å.

	a	b	c	d	e	ρ
TCNQ ^{1,2}	1.355	1.433	1.396	1.424	1.145	0.5
TCNQ A	1.346	1.437	1.378	1.431	1.140	0.14 (6)†
TCNQ B	1.361	1.419	1.412	1.416	1.142	0.86 (6)†

* Ashwell, Wallwork, Baker & Berthier (1975).

† After normalization.

Chasseau (1977), with the normalization condition $\rho(A) + \rho(B) = 1$. In this calculation, for each TCNQ molecule the bond lengths are averaged with the assumption of mmm symmetry. For example, Table 3 gives the relevant room-temperature data for DMM(TCNQ)₂(II), the structure with the largest $|\Delta\rho|$.

The 'disordered groups' column shows that disorder of the cations is a frequent phenomenon. From measurements of diffuse X-ray scattering as a function of temperature, it could be deduced that, with the exception of HBTM(TCNQ)₂ (Visser, van Smaalen, de Boer & Vos, 1990), the disorder is primarily dynamic.

The lower part of Fig. 1 illustrates a common feature of the present TCNQ salts: the occurrence of sheets of parallel TCNQ stacks containing electrostatically favourable interstack $N \cdots H$ contacts, down to 2.63 Å for this example. This tendency to pseudo-two-dimensional character has an impact on the physical properties. For MEM(TCNQ)₂, for instance, it becomes apparent from the anisotropy of the electrical conductivity σ at room temperature: $\sigma(\text{in sheet, } \parallel \text{ stack}) : \sigma(\text{in sheet, } \perp \text{ stack}) : \sigma(\perp \text{ sheet}) = 40:8:1$ (Almeida, Alcacer & Oostra, 1984). In general, the crystals contain 'flat' sheets, successive sheets being separated by a layer of cations, as shown in Fig. 1. There is one exception: DMM(TCNQ)₂(II). As can be seen from Fig. 3, in this compound the sheets are corrugated, successive sheets come close together and the cations are packed in channels along the stacks. It is noteworthy that this exceptional sheet structure is accompanied by a strong charge localization (Table 2).

In most compounds, the stacks in successive sheets are parallel. Exceptions are the so-called 'crossed-chain' compounds: HMM(TCNQ)₂ and DEM(TCNQ)₂. In HMM(TCNQ)₂, successive sheets are related by a 4_1 axis perpendicular to the sheets; consequently, the angle between the crossed chains is

90°. DEM(TCNQ)₂ has two inequivalent sheets per cell, the stacks in successive sheets making an angle of ~60° with each other (Fig. 4).

Phase transitions

In Table 4, the phase transitions of [RR'(T)M](TCNQ)₂ compounds studied by crystallographic means are summarized. It turns out that only MEM(TCNQ)₂ shows the two phase transitions (4 kF, uniform → dimeric chains; 2 kF, dimeric → tetrameric chains) predicted by consideration of the elec-

tronic behaviour of the stacks (Huizinga, Kommandeur, Jonkman & Haas, 1982). Table 4 illustrates that, apart from the 17.4 K transition of MEM(TCNQ)₂, it is not only the electronic nature of the stacks that induces the phase transition. Changes in the dynamic disorder of the cations also play an important role [for extensive studies, see Oostra, van Bodegom, Huizinga, Sawatzky, Grüner & Travers (1981) and Almeida, Alcacer & Oostra (1984)]. A further illustration of the influence of the cations is the suppression of the 4 kF transition in MEM(TCNQ)₂ through doping with METM; if approximately one in five MEM cations are randomly replaced by METM, the transition is no longer detected (van Smaalen, de Boer & Kommandeur, 1985). Another extreme example is the second-order phase transition of DMM(TCNQ)₂(II). This transition hardly influences the stacks but leads to an incommensurate long-range ordering of the DMM groups at low temperatures (Steurer, Visser, van Smaalen & de Boer, 1987).

The phase transitions of monoclinic DMM(TCNQ)₂(I) and of DMTM(TCNQ)₂ exemplify the transformations to completely different low-temperature structures of compounds that are isomorphous at room temperature. At room temperature, the cations in the two isomorphous crystals are disordered around the mirror planes of their space group $P2_1/m$. In both cases, these mirror planes vanish as a result of ordering of the cations when the crystals are cooled. The resulting low-temperature structures have, however, different space groups and different stack characteristics. In the monoclinic low-temperature phase of DMM(TCNQ)₂(I), Z is four times larger than at room temperature and the stacks are octameric. However, at the transition to the low-temperature phase of DMTM(TCNQ)₂, Z remains the same, the symmetry is reduced to triclinic and the two sheets in the cell become inequivalent. The inequivalence of the sheets has a strong impact on the physical properties. On cooling the DMTM(TCNQ)₂ crystals, the conductivity σ increases by about a factor of 500 at the phase transition. This unexpected phenomenon has been explained by assuming that the inequivalent crystal potentials at alternating sheets cause a strong reduction in the energy gap for electron transfer between the sheets (Visser, van Smaalen, de Boer & Vos, 1985; Almeida, Alcacer, Oostra & de Boer, 1987).

Predictability of [RR'(T)M](TCNQ)₂ structures

Table 2 shows that chemically small modifications of the cations, such as substitution of sulfur for oxygen are generally accompanied by strong changes in the [RR'(T)M](TCNQ)₂ structures. Striking

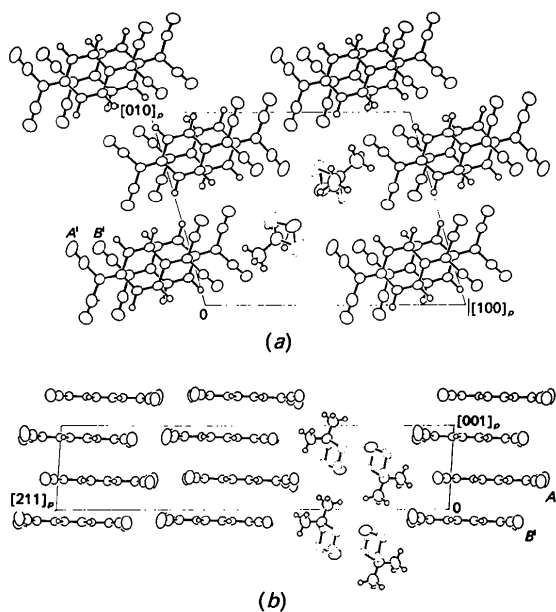


Fig. 3. Projections of the structure of DMM(TCNQ)₂(II) at room temperature (from Visser, 1984). Each dashed C atom of the disordered DMM groups represents two fractional atoms; the subscript p denotes the projected direction. (a) Along [001] onto the plane perpendicular to [001]; (b) normal projection of one layer of TCNQ and DMM groups along the molecular axis M defined in Fig. 2.

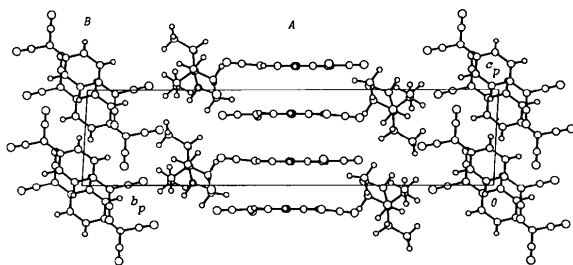


Fig. 4. Projection of the structure of DEM(TCNQ)₂ along [100] onto the plane perpendicular to [100] (from Morssink & van Bodegom, 1981); the subscript p denotes the projected axis. Two inequivalent sheets consisting of stacks A-A- and B-B-, respectively, can be distinguished.

Table 4. Phase transitions in $[RR'(T)M](TCNQ)_2$ compounds for which crystallographic evidence is available

See Table 2 for structure determinations. σ ($\Omega^{-1} \text{ cm}^{-1}$) is the electrical conductivity; ES (eV) is the slope of the $-\ln\sigma$ versus $1/kT$ curve; μ is the mobility of charge carriers.

Cation	T (K)	Stack	Disorder/remarks	σ /ES/ μ	Reference
MEM	> 338 ^a	Almost uniform	Vigorous MEM rotations about two axes ^b	$\sigma(340 \text{ K}) = 30$, ES = 0	1
	< 338	Strongly dimeric	Strong restricted MEM rotation; $x(323 \text{ K}) = 0.63^c$	ES = 0.33 (2)	1
	314 ^a	Strongly dimeric	Strong decrease in rotation (second-order transition ^a)		2
	314–280	Strongly dimeric	MEM rotation vanishes gradually, $x(\text{RT}) = 0.84$	$\mu(280 \text{ K}); \mu(314 \text{ K}) = 1:3.5^d$, ES = 0.8 ^e , $\sigma(\text{RT}) = 1.5 \times 10^{-3}$	1, 3
DMTM	< 280	Strongly dimeric	$x(113 \text{ K}) = 1$	ES = 0.32 (2)	1
	< 17.4	Slightly tetrameric			
DMM(I)	> 272	Strongly dimeric	Dynamic DMTM disorder at m	$\sigma(273 \text{ K}) = 6 \times 10^{-3}$, ES = 0.26	4
	< 272	(e)	Two independent sheets ^e	$\sigma(271 \text{ K}) = 3$, ES = 0.036	4
DMM(II)	> 260	Strongly dimeric	Dynamic DMM disorder at m	$\sigma(\text{RT}) = 2.0 \times 10^{-2}$, ES = 0.23	5
	< 260	Octameric	DMM ordered		
DMM(II)	> 200	Almost uniform	DMM dynamic chair-to-chair disorder	$\sigma(\text{RT}) = 5.6 \times 10^{-5}$ (strong charge localization)	5
	200–150	Almost uniform	Increasing incommensurate DMM long-range order		

Notes: (a) Discontinuous change in thermoelectric power (TEP) measurements at 338 K and TEP anomaly at 314 K (Almeida, Alcacer & Oostra, 1984). (b) From NMR measurements (Oostra, van Bodegom, Huizinga, Sawatzky, Grüner & Travers, 1981). (c) x and $1-x$ are the occupancies of the two preferred orientations, from X-ray diffraction. (d) Alternative interpretation of anomalous slope: change in activation energy E_a by $d(E_a)/dT = -9 \times 10^{-4} \text{ eV K}^{-1}$, giving $\Delta(E_a) = E_a(314 \text{ K}) - E_a(280 \text{ K}) = -0.03 \text{ eV}$, to be compared with $\Delta(\text{ES}) = 0.01(3) \text{ eV}$. (e) Indirect evidence from reflection symmetry and cell constants, symmetry changes from $P2_1/m$ ($Z = 2$) above 272 K (Visser, de Boer & Vos, 1990b) to triclinic ($Z = 2$) below 272 K; according to ESR measurements the low-temperature phase contains crossed chains with interchain angle $\sim 25^\circ$ (Kirui, Ma, Weih & Schwerdtfeger, 1990).

References for physical properties: (1) Oostra, van Bodegom, Huizinga, Sawatzky, Grüner & Travers (1981). (2) Almeida, Alcacer & Oostra (1984). (3) van Bodegom (1981, Fig. 1). (4) Almeida, Alcacer, Oostra & de Boer (1987). (5) Oostra (1985).

examples are: (1) packing, as well as tetramerization of the stacks, is strongly different in EBM(TCNQ)₂ and EBTM(TCNQ)₂; (2) there is no analogy between the low-temperature phases of DMM(TCNQ)₂(I) and DMTM(TCNQ)₂; (3) substitution of CH₃ for the somewhat more bulky C₂H₅ group in HEM(TCNQ)₂ leads to the completely different structure of HMM(TCNQ)₂, in which successive sheets are rotated through an angle of 90°. These examples emphasize the impossibility of inducing predictable changes in stack and sheet structure by (small) chemical modifications of the cations.

Physical properties

Introduction

The electronic properties of TCNQ salts and other quasi-one-dimensional materials are usually discussed in terms of the extended Hubbard (1978) model. Within the framework of this model, the physical properties depend on the following parameters: (1) the transfer integrals $t(i)$ for hopping of electrons from site i to site $i + 1$; (2) the Coulomb repulsion U between two electrons with paired spins residing at the same site; (3) the Coulomb repulsion $V(n)$ between electrons at sites i and $i + n$; and (4) the electrostatic potential $+\Delta$ at A and $-\Delta$ at B , if the model is generalized to two inequivalent TCNQ's A and B per translation period. For $U = \Delta = V = 0$, the bandwidth is $4t$ for regular chains with transfer integral t . The parameters U , t and V assume effective

values. For example, U will be affected by polarization of the embedding lattice (Sawatzky, Kuindersma & Kommandeur, 1975) and, to an extent depending on the band filling, by the approximations made in the theory, such as neglect of long-range repulsions (Mazumdar & Bloch, 1983). In many cases $V(n)$ is neglected or only roughly accounted for by considering $V(1)$ with effective value:

$$V(1; \text{eff}) \equiv V = V(1) - V(2). \quad (3)$$

The $[RR'(T)M](TCNQ)_2$ compounds belong to the group of organic conductors with $U \gg 4t$ (Mazumdar & Bloch, 1983). The large U makes doubly occupied states unfavourable. The lower band, available for the electrons, consists of singly occupied states only. Hence, the chains have a large magnetic susceptibility compared with metals. The electrical conductivity of an $[RR'(T)M](TCNQ)_2$ salt, with 0.5 e charge per TCNQ and thus a half-filled lower band, is expected to depend strongly on the band gap $E(g)$ at the Fermi level. Physical characteristics are given in Table 5. In Table 6 experimental and theoretical quantities are compared.

Magnetic susceptibility $\chi(T)$

In Groningen, magnetic susceptibilities $\chi(T)$ have been obtained by integrating the calibrated electron spin resonance signal (Huizinga, 1980; Oostra, 1985). The curves turned out to be different for the different (sub)classes of Table 2. In the present paper, the

Table 5. *Physical characteristics for [RR'(T)M](TCNQ)₂ complexes*

Parameters Δ , U and V

Δ (Table 6) obtained from $\Delta\rho$ (Table 2) by theoretical calculations on finite chains with neglect of V (Oostra, 1985); $U = 1.4$ (Mazumdar & Soos, 1981), $V = 0.4$ eV (Oostra, 1985).

Class I compounds

Band gap* (Oostra, 1985):

$$E(g) = 2\{[t(1) - t(2)]^2 + \Delta^2\}^{1/2}. \quad (T1)$$

Electrical conductivity (class I and II):

$$\sigma = n^+ e \mu \exp(-E(g)/2kT) \quad (T2)$$

n^+ = number of charge carriers; e = charge electron; μ = mobility.

Spin Hamiltonian (uniform antiferromagnetic exchange):

$$\hat{H} = 2J \sum_i S(i)S(i+1). \quad (T3)$$

Summation over all lowest-unoccupied-molecular-orbital electrons; J = exchange integral, $S(i)$ = spin operator for $S(i) = 1/2$.

Magnetic susceptibility $\chi(T)$:

Bonner & Fischer (1964) model for antiferromagnetic Heisenberg coupling; the magnetic energy spectrum is gapless so $\chi(T) \neq 0$ for $T \rightarrow 0$, implying that class I compounds are thermodynamically unstable for $T \rightarrow 0$. For $T \geq 1.0 \times J$, susceptibility is given by:

$$J\chi/Ng^2\mu(B)^2 = 0.25\{[T/J + 1]\{1 - 1/[1.056(T/J)^2 + 1.3]\}\}. \quad (T4)$$

Class II compounds

Band gap (Oostra, 1985):

$$E(g) = [t(AA) + t(BB) - (1/2)\{[t(BB) - t(AA) - 2\Delta]^2 + 4t(AB)^2\}^{1/2} - (1/2)\{[t(BB) - t(AA) + 2\Delta]^2 + 4t(AB)^2\}^{1/2}]. \quad (T5)$$

Spin Hamiltonian (alternating antiferromagnetic exchange):

$$\hat{H} = 2\sum_i [J_1 S(2i)S(2i+1) + J_2 S(2i+1)S(2i+2)], \quad (T6)$$

with $J_1 > J_2$.

Magnetic susceptibility (singlet-triplet model):

$$\chi(T) = Ng^2\mu(B)^2/kT[3 + \exp(\Delta E)/kT]^{-1}. \quad (T7)$$

$$\text{Gap: } \Delta E \approx 2\Delta J \approx 2(J_1 - J_2), \quad \chi(T) \rightarrow 0 \text{ for } T \rightarrow 0. \quad (T8)$$

* With neglect of $V(n)$. For uniform chains, $U \rightarrow \infty$ and $\Delta = 0$, band gaps due to $V(1, \text{eff}) = V$ start to occur for $V/2t > 1$ (Ovchinnikov, 1973). For the present choice of parameters, such V gaps are expected to be very small. Theoretical estimates of the influence of V on gaps are not available for strongly dimeric chains.

discussion is restricted to $\chi(T)$ curves of compounds with known crystal structures.

According to Oostra (1985) the $\chi(T)$ values of crystals of class I(1, d , p) can generally be fitted to the Bonner-Fischer model (Table 5), if a small temperature dependence of J is taken into account: $(1/J)dJ/dT$ varies from 0 to $-0.5 \times 10^{-3} \text{ K}^{-1}$ at room temperature. An exception is DMM(TCNQ)₂(II); J is low for the high-temperature structure because of the strong charge localization at alternate sites and turns out to be modulated along the stacks in the low-temperature structure because of the incommensurable modulation of the cations (Kramer & Brom, 1988). In HBTM(TCNQ)₂, class I(1, s , p), which shows static disorder of the cations, $\chi(T)$ deviates from the Bonner-Fischer model because the stacks are locally tetrameric and contain kinks. In class I(2, d , p) $\chi(T)$ is the superposition of the susceptibilities of the two inequivalent stacks (Oostra, 1985). The crossed chain compounds DEM(TCNQ)₂ and HMM(TCNQ)₂ show a remarkably large angular anisotropy in the

susceptibility for each stack (Schwerdtfeger, Oostra & Sawatzky, 1982; Oostra, Visser, Sawatzky & Schwerdtfeger, 1983). According to Cabanas & Schwerdtfeger (1989), this anisotropy is caused by a very weak (J equal to a few 0.01 K) antiferromagnetic coupling between each of the spins on the adjacent nonparallel stacks.

For class II, adjustment of $\chi(T)$ to (T7) (Table 5) turned out to be possible with the assumption of a relatively large temperature dependence of ΔJ ; at room temperature, $(1/\Delta J)d\Delta J/dT$ (K^{-1}) is -3.1×10^{-3} for EBM(TCNQ)₂, -2.4×10^{-3} for HEM(TCNQ)₂ and -1.4×10^{-3} for EBTM(TCNQ)₂ (Huizinga, 1980; Oostra, 1985). This large temperature dependence indicates that tetramerization of the stacks increases with decreasing T , especially for EBM(TCNQ)₂ and HEM(TCNQ)₂. The $\chi(T)$ curve of the former compound suggests that tetramerization sets in rapidly below 260 K.

Exchange integrals J at room temperature

The experimental $J(\text{exp})$ and $\Delta J(\text{exp})$ values in Table 6 are deduced from the measured susceptibilities by the use of (T4) and (T7), respectively. The theoretical $J(\text{th})$ and $\Delta J(\text{th})$ values are obtained through calculations based on the full Hubbard Hamiltonian including intersite repulsion (V) and the lattice potential Δ (Oostra, 1985). In view of the experimental values, three categories are distinguished.

(1) DMM(TCNQ)₂(II). $J(\text{exp})$ is very low because of the strong charge localization at alternate sites along the stacks. The discrepancy between $J(\text{exp})$ and $J(\text{th})$ suggests that the theory underestimates the influence of charge localization.

(2) Class II compounds. For the pronounced tetrameric compounds HEM(TCNQ)₂ and EBTM(TCNQ)₂, $\Delta J(\text{exp})$ is high because of the strong charge accumulation at neighbouring sites at the centre of a tetramer [Table 2; Fig. 8 in the paper of Huizinga, Kommandeur, Jonkman & Haas (1982)]. According to Oostra (1985, 1991) $\Delta J(\text{exp})$ is lowered because of relaxation of the actual *dynamic* lattice after triplet formation. Nevertheless, the agreement between $\Delta J(\text{exp})$ and $\Delta J(\text{th})$ calculated for a *static* lattice is good, presumably because the theory does not completely account for the enhancement of ΔJ by the charge accumulation. For EBM(TCNQ)₂, the time-averaged structure of the stacks is almost uniform, but low-frequency thermal modes anticipating the tetramerization below 260 K will induce small-timescale tetrameric features. Analysis of $\chi(T)$ at room temperature with (T4) gives $J \approx 140$ K, whereas (T7) leads to $J(1) - J(2) \approx 200$ K.

(3) Class I compounds except DMM(TCNQ)₂(II). $J(\text{exp})$ shows intermediate values that do not vary

Table 6. *Physical properties of [RR'(T)M](TCNQ)₂ compounds at room temperature*

$t(2)$, Δ , $E(g)/2$ and ES are in eV; $J(\text{exp})$ and $J(\text{th})$ are the experimental and calculated exchange integrals (in K), respectively; 2Δ is the electrostatic potential difference between inequivalent molecules in a stack; $E(g)$ is the calculated band gap; σ is the electrical conductivity (in $\Omega^{-1} \text{cm}^{-1}$); ES is the slope of the $-\ln\sigma$ versus $1/kT$ curve at RT; ES(LT) (in K) is the corresponding slope at low temperature. E.s.d.'s, in parentheses, of Δ and $E(g)/2$ are deduced from the e.s.d. of $\Delta\rho$ (Table 2). The MEM(TCNQ)₂ conductivity is taken from Table 4, the remaining data from Oostra (1985).

Class I	Cation	$t(2)$	$J(\text{exp})^a$	$J(\text{th})$	Δ	$E(g)/2$	σ^b	ES	ES(LT)	
(1,d,p)	MBTM	0.17	81'	197	0.05 (4)	0.05 (4)	9	~0	0.17 (~200 K)	
	METM	0.18	80'	211	0.07 (1)	0.07 (1)	4	~0	0.08 (~200 K)	
	DMM(I)	0.06	82	33		0.12	2.0×10^{-2}	0.23		
	DMTM	0.04	42	16		0.14	1.4×10^{-2}	0.26		
	MEM	0.06	53	26	0.05 (5)	0.15 (1)	1.5×10^{-3}	Table 4		
	DMM(II)	0.11	9	53	0.17 (2)	0.17 (2)	5.6×10^{-5}	0.29		
	(1,d,c)	HMM	0.16	140'	178	0.08 (2 _s)	0.08 (2 _s)	1.7×10^{-1}	0.17	0.10 (100 K)
	(1,s,p)	HBTM	0.15					1.7×10^{-1}	0.11	
	(2,d,p)	MBM	0.17 ^d	63 ^e	190 ^e		< 0.01 ^d	9	~0	0.07 (~200 K)
	(2,d,c)	MPM	0.16 ^d	73 ^e	168 ^e		0.02 ^d	1.2×10^{-1}	0.05	
	DEM	0.04 ^d	64 ^e	12 ^e		0.15 ^d	3.7×10^{-3}	0.09		
Class II	Cation	$t(BB)$	$\Delta J(\text{exp})$	$\Delta J(\text{th})$	Δ	$E(g)/2$	σ	ES		
(1,d,p)	EBM	0.17	(f)	-	< 0.01	0.01	3.5×10^{-2}	0.06		
	HEM	0.19	435	397	0.08 (1)	0.06 (1)	3.2×10^{-2}	0.37		
	EBTM	0.13	215	224	0.08 (1 _s)	0.16	1.7×10^{-4}	0.20		

Notes: (a) Error class I $J(\text{exp})$ values ± 5 K. (b) Uncertainties due to crystal cracking and hysteresis. (c) Values determined from $\chi(T)$ maxima are 80 (MBTM and METM) and 170 K (HMM). (d) Chain with lower $E(g)$ given. (e) 'Average' value for two inequivalent stacks. (f) See text.

systematically with the smaller transfer integral $t(2)$. For the strongly dimeric compounds, $J(\text{exp})$ is larger than $J(\text{th})$, the increase corresponding to a $t(2)$ increase of ~ 0.02 eV. The almost uniform chain compounds can be divided into two groups: (a) METM(TCNQ)₂, MBTM(TCNQ)₂, MBM(TCNQ)₂ and MPM(TCNQ)₂, which have strongly analogous overall crystal packings [for an example, see Fig. 3 in the paper by Visser, de Boer & Vos (1990a)] and $J(\text{exp})$ values that are considerably lower than $J(\text{th})$; (b) HMM(TCNQ)₂, which has a strongly different crystal packing [Fig. 2 in the paper by Visser, de Boer & Vos (1990c)] and a $J(\text{exp})$ value that is not much smaller than $J(\text{th})$. This indicates that $J(\text{exp})$ does not depend only on the stacks, but also on the crystal packing as a whole. In our opinion, major effects to be considered in future discussions are lattice relaxation (Oostra, 1991) and deformation of conduction-band orbitals by the crystal field. The assumed existence of the latter effect is supported by the fact that the ¹³C NMR Knight shifts for the CN groups in DMTM(TCNQ)₂ at room temperature are not equal, but vary from -600 to -900 (in 10^{-6}) (Rachdi, Bernier, Nunes, Ribet & Almeida, 1991).

Electrical conductivity

In Table 6, the compounds of each class are ordered according to their electrical conductivity σ along the stacks (Oostra, 1985). Within each class, σ is found to decrease with increasing calculated band gap $E(g)$, as expected. The $\sigma, E(g)$ pair of HMM(TCNQ)₂ fits into the sequence of class I (1,d,p). It must be noted, however, that for most of the compounds Table 6 shows a pronounced difference between the theoretical activation energy $E(g)/2$ and the slope, ES, of the $-\ln\sigma$ versus $1/kT$ curve. This

emphasizes that for the present dynamic lattices, temperature-dependent quantities other than $E(g)/2$ have a strong impact on σ . The following features can be noticed:

(1) Decrease of the mobility, μ , with T ('metallic' behaviour; ES=0) for compounds with $\sigma \geq 4\Omega^{-1} \text{cm}^{-1}$. At low temperatures (LT) the conductivity is thermally activated [ES(LT) > 0].

(2) Strong increase in ES [ES > $E(g)/2$] owing to strong increase of dynamic cation disorder with T . This phenomenon has been studied extensively for MEM(TCNQ)₂ (Table 4, interval 314–280 K). A further possible example is HEM(TCNQ)₂.

(3) Scattering of charge carriers by thermal modes [example EBM(TCNQ)₂]. Starting from room temperature, the amplitudes of the low-frequency modes anticipating the tetramerization below 260 K increase with decreasing T . The corresponding increase in the scattering reduces σ with decreasing T , resulting in an increase of the slope ES [ES > $E(g)/2$].

(4) Reduction of the charge transfer between inequivalent stacks with increasing T [example DEM(TCNQ)₂]. The increase in thermal motion and DEM disorder with T reduces the potential difference and thus the charge transfer between inequivalent stacks. This effect decreases σ with increasing T and causes a lowering of the slope ES [ES < $E(g)/2$].

The phenomena discussed above show that the electrical conductivity does not depend only on the structure of the stacks, but also on the interaction between charge carriers and the *dynamic* lattice as a whole. Therefore, further quantitative interpretation of the σ values listed in Table 6 is considered impossible.

Concluding remarks

The $[RR'(T)M](TCNQ)_2$ complexes described in the present paper show strong variety in their electrical conductivities and magnetic susceptibilities. Strong interplay between crystal structure determinations, physical measurements and theoretical modelling has been necessary to understand the essential features of these properties and to describe the numerous phase transitions. In spite of this gain in physical knowledge, it has turned out to be impossible to design crystals with desired physical properties, as was hoped for at the beginning of this research. The fundamental bottleneck lies in the structural evidence discussed earlier: that chemically small modifications of the cations generally cause large unpredictable changes in crystal structure. For organic conductors of the $[RR'(T)M](TCNQ)_2$ class, it must, therefore, be concluded that the discovery of a compound with *a priori* desired behaviour is the result of serendipity rather than systematic research.

We thank Dr S. Oostra and Professor Dr J. Kommandeur for critical reading of the manuscript and valuable discussions.

References

- ALMEIDA, M., ALCACER, L. & OOSTRA, S. (1984). *Phys. Rev. B*, **30**, 2839–2844.
- ALMEIDA, M., ALCACER, L., OOSTRA, S. & DE BOER, J. L. (1987). *Synth. Met.* **19**, 445–450.
- ASHWELL, G. J., WALLWORK, S. C., BAKER, S. R. & BERTHIER, P. I. C. (1975). *Acta Cryst.* **B31**, 1174–1178.
- BODEGOM, B. VAN (1981). *Acta Cryst.* **B37**, 857–863.
- BODEGOM, B. VAN & DE BOER, J. L. (1981). *Acta Cryst.* **B37**, 119–125.
- BODEGOM, B. VAN & BOSCH, A. (1981). *Acta Cryst.* **B37**, 863–868.
- BONNER, J. C. & FISCHER, M. E. (1964). *Phys. Rev.* **135**, A640–658.
- BOSCH, A. & VAN BODEGOM, B. (1977). *Acta Cryst.* **B33**, 3013–3021.
- CABANAS, F. X. & SCHWERDTFEGER, C. F. (1989). *Phys. Rev. B*, **39**, 11241–11250.
- FLANDROIS, S. & CHASSEAU, D. (1977). *Acta Cryst.* **B33**, 2744–2750.
- HUBBARD, J. (1978). *Phys. Rev. B*, **17**, 494–505.
- HUIZINGA, S. (1980). Thesis, Univ. of Groningen, The Netherlands.
- HUIZINGA, S., KOMMANDEUR, J., JONKMAN, H. T. & HAAS, C. (1982). *Phys. Rev. B*, **25**, 1717–1725.
- KAMMINGA, P. & VAN BODEGOM, B. (1981). *Acta Cryst.* **B37**, 114–119.
- KIRUI, J. K., MA, C. L., WEIH, D. & SCHWERDTFEGER, C. F. (1990). *Solid State Commun.* **74**, 451–453.
- KRAMER, G. J. & BROM, H. B. (1988). *J. Phys. C*, **21**, 5435–5448.
- MAZUMDAR, S. & BLOCH, A. N. (1983). *Phys. Rev. Lett.* **50**, 207–211.
- MAZUMDAR, S. & SOOS, Z. G. (1981). *Phys. Rev. B*, **23**, 2810–2823.
- MIDDELDORP, J. A. M., VISSER, R. J. J. & DE BOER, J. L. (1985). *Acta Cryst.* **B41**, 369–374.
- MORSSINK, H. & VAN BODEGOM, B. (1981). *Acta Cryst.* **B37**, 107–114.
- OOSTRA, S. (1985). Thesis, Univ. of Groningen, The Netherlands. Unpublished paper.
- OOSTRA, S., VAN BODEGOM, B., HUIZINGA, S., SAWATZKY, G. A., GRÜNER, G. & TRAVERS, J. P. (1981). *Phys. Rev. B*, **24**, 5004–5013.
- OOSTRA, S., VISSER, R. J. J., SAWATZKY, G. A. & SCHWERDTFEGER, C. F. (1983). *J. Phys. (Paris)*, **44**, 1381–1382.
- OVCHINNIKOV, A. A. (1973). *Sov. Phys. JETP*, **37**, 176–177.
- RACHDI, F., BERNIER, P., NUNES, T., RIBET, M. & ALMEIDA, M. (1991). *Synth. Met.* **41–43**, 1869–1872.
- RICE, M. J., YARTSEV, V. M. & JACOBSEN, C. S. (1980). *Phys. Rev. B*, **21**, 3437–3446.
- SAWATZKY, G. A., KUINDERSMA, P. I. & KOMMANDEUR, J. (1975). *Solid State Commun.* **17**, 569–571.
- SCHWERDTFEGER, C. F., OOSTRA, S. & SAWATZKY, G. A. (1982). *Phys. Rev. B*, **25**, 1786–1790.
- SMAALEN, S. VAN, DE BOER, J. L. & KOMMANDEUR, J. (1985). *Mol. Cryst. Liq. Cryst.* **120**, 173–177.
- SMAALEN, S. VAN & KOMMANDEUR, J. (1985). *Phys. Rev. B*, **31**, 8056–8060.
- STEURER, W., VISSER, R. J. J., VAN SMAALEN, S. & DE BOER, J. L. (1987). *Synth. Met.* **B43**, 567–574.
- VISSER, R. J. J. (1984). Thesis, Univ. of Groningen, The Netherlands.
- VISSER, R. J. J., BOUWMEESTER, H. J. M., DE BOER, J. L. & VOS, A. (1990a). *Acta Cryst.* **C46**, 852–856.
- VISSER, R. J. J., BOUWMEESTER, H. J. M., DE BOER, J. L. & VOS, A. (1990b). *Acta Cryst.* **C46**, 860–864.
- VISSER, R. J. J., DE BOER, J. L. & VOS, A. (1990a). *Acta Cryst.* **C46**, 857–860.
- VISSER, R. J. J., DE BOER, J. L. & VOS, A. (1990b). *Acta Cryst.* **C46**, 864–866.
- VISSER, R. J. J., DE BOER, J. L. & VOS, A. (1990c). *Acta Cryst.* **C46**, 869–871.
- VISSER, R. J. J., OOSTRA, S., VETTER, C. & VOIRON, J. (1983). *Phys. Rev. B*, **28**, 2074–2077.
- VISSER, R. J. J., VAN SMAALEN, S., DE BOER, J. L. & VOS, A. (1985). *Mol. Cryst. Liq. Cryst.* **120**, 167–172.
- VISSER, R. J. J., VAN SMAALEN, S., DE BOER, J. L. & VOS, A. (1990). *Acta Cryst.* **C46**, 867–869.